Selective Step-Growth Phenol–Aldehyde Polymerization. 3.[1] Synthesis, Characterization, and X-ray Analysis of Regular All-Ortho Ethylidene-Linked Oligonuclear Phenolic Compounds

Giovanni Casiraghi,*[2a] Mara Cornia,[2a] Giovanni Ricci,[2a] Giuseppe Casnati,[2a] Giovanni D. Andreetti,[2b] and Lucia Zetta[2c]

Istituto di Chimica Organica dell'Università, I-43100 Parma, Italy, Istituto di Strutturistica Chimica dell'Università and Centro di Studio per la Strutturistica Diffrattometrica del CNR, I-43100 Parma, Italy, and Istituto di Chimica delle Macromolecole del CNR, I-20130 Milano, Italy. *Received February 23, 1983*

ABSTRACT: All-ortho phenol–acetaldehyde novolac resins with uniform constitution were prepared via bromomagnesium ion mediated reaction of phenol with acetaldehyde derivatives. Rational regio- and stereocontrolled syntheses of some oligonuclear all-ortho ethylidene-linked phenolic compounds were also described by reaction of suitable phenoxymagnesium bromide precursors in benzene with acetaldehyde, acetaldehyde diethyl acetal, or *rac*-2-hydroxy-α-methylbenzyl alcohol. The prepared pure binuclear (**2**), trinuclear (*meso*- and *rac*-**3m** and -**3r**), tetranuclear (syndiotactic and atactic **4rr** and **4mr**), and pentanuclear (syndiotactic **5rrr**) oligomers were separated by chromatographic methods and fully characterized by combined IR, UV, mass, ^{1}H NMR, and ^{13}C NMR spectroscopy. Single-crystal X-ray structural analysis of trinuclear compounds **3m** and **3r** reveals that, in the solid state, the conformation of these molecules is mainly determined by the isodromic intramolecular hydrogen-bond system, running on opposite sides of the ethylidene methyl groups.

Introduction

In previous papers of this series[1,3] we have developed a novel and potentially general approach to control the regiochemistry of the phenol–formaldehyde polycondensation using bromomagnesium ion driven reactions of suitable phenolic precursors with formaldehyde or salicyl alcohol. Complexation of both the phenolic substrate and the reagent to the metal atom leads to regiochemical control typical of an intramolecular metal-mediated alkylation process.

The success of this approach strictly depends on the nature of the catalyst and the solvent, reaching the maximum ortho specificity when highly coordinating metal ions ($MgBr^+$, Zn^{2+}) and aprotic nonpolar reaction media such as benzene or toluene are used.[3,4]

In this context, the extension of this method to aldehydes other than formaldehyde[5] assumes great synthetic and theoretical relevance if both the regiochemistry and stereochemistry of the process are controllable. The present paper reports a detailed study on the regio- and stereocontrolled reactions of phenol with acetaldehyde and related reagents leading to regular all-ortho ethylidene-polyphenols (acetaldehyde novolacs) and deals with the synthesis, separation, characterization, and X-ray structural analysis of some produced low molecular weight oligomers. Ortho–ortho′ ethylidene-linked oligonuclear phenolic compounds in this report represent a class of substances that has received only marginal attention until now.[6]

Results and Discussion

Synthesis of All-Ortho Acetaldehyde Novolacs. The reaction of the bromomagnesium salt of phenol in refluxing benzene with acetaldehyde (0.5 mol equiv) followed by acidic quenching and routine workup afforded a solid material melting between 60 and 80 °C in very high yield (>90% based on phenol). Reverse-phase liquid chromatography analysis on a μ-Bondapak C-18 column using a methanol/water solvent system (Figure 1) revealed that this material was a mixture of six major components, later identified as all-ortho ethylidene-linked binuclear oligomer **2** (47%), racemic trinuclear oligomer **3r** (24%), meso trinuclear oligomer **3m** (11%), atactic tetranuclear oligomer **4mr** (or **4rm**) (5%), syndiotactic tetranuclear oligomer **4rr** (3%), and syndiotactic pentanuclear oligomer **5rrr** (1%) (Chart I).

Chart I

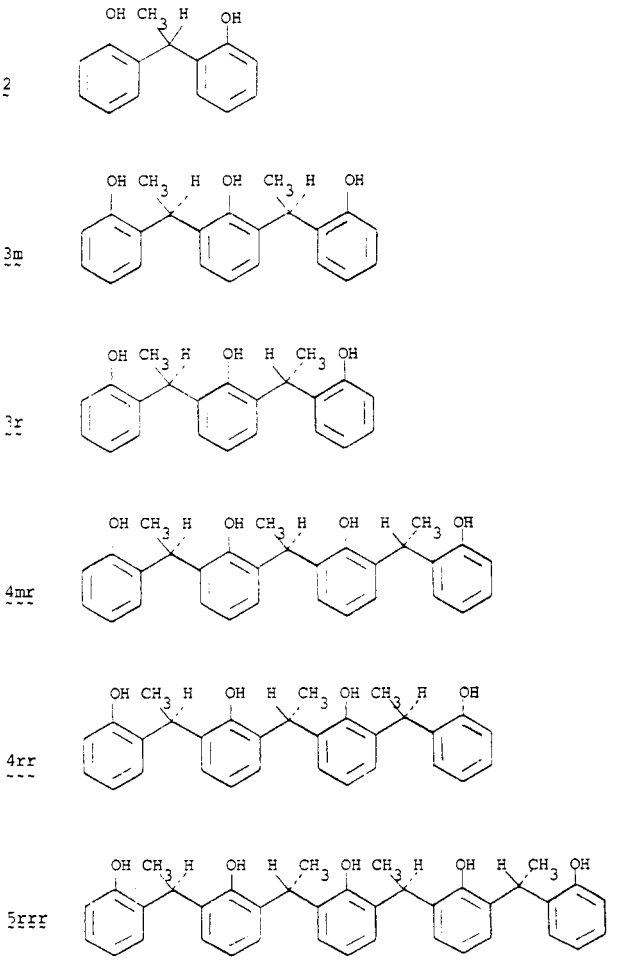

The quantitation was directly made by peak area measurements on the HPLC chromatogram monitored at 280 nm as previously described for the analysis of all-ortho phenol–formaldehyde novolac resins.[7] Separation of all

0024-9297/84/2217-0019$01.50/0

Table I
Analytical and Physical Data of All-Ortho Ethylidene-Linked Oligonuclear Phenolic Compounds

compd	mp, °C (recrystn solv)	formula (fw)	anal.: found (calcd) % C	% H	HPLC R_t,[a] min	TLC R_f[b] A	B
2	114 (hexane/acetone)	$C_{14}H_{14}O_2$ (214.25)	78.18 (78.48)	6.40 (6.59)	5.58	0.15	0.29
3r	120 (benzene/cyclohexane)	$C_{22}H_{22}O_3$ (334.40)	79.20 (79.01)	6.73 (6.63)	8.43	0.16	0.23
3m	157-158 (hexane/acetone)	$C_{22}H_{22}O_3$ (334.40)	78.72 (79.01)	6.58 (6.63)	8.68	0.21	0.27
4rm	155 (benzene)	$C_{30}H_{30}O_4$ (454.54)	79.35 (79.27)	6.72 (6.65)	14.08	0.27	0.22
4rr	165 (benzene)	$C_{30}H_{30}O_4$ (454.54)	79.10 (79.27)	6.62 (6.65)	15.08	0.24	0.20
5rrr	149-150 (hexane)	$C_{38}H_{38}O_5$ (574.68)	79.36 (79.41)	6.63 (6.67)	20.25	0.29	0.14

[a] Conditions: column, μ-Bondapak C-18, 30 cm × 7.8 mm (internal diameter); mobile phase, 80:20 (v/v) methanol/water; flow rate, 3.5 mL/min; back pressure, 1500 psi. [b] Conditions: Stratochrom SIF silica gel precoated plates; eluent A, chloroform (0.3% ethanol); eluent B, 80:20 (v/v) hexane/acetone.

Table II
Reactions of Metal Phenolates with Acetaldehyde under Various Conditions[a]

expt	metal ion	additive (equiv)	solvent	yield of resin,[b] %	composition,[c] % 2	3m	3r	4mr	4rr	5rrr
1	$MgBr^+$	none	benzene	91	51.6	12.1	26.4	5.5	3.3	1.1
2	Li^+, Na^+, K^+	none	benzene	no reaction						
3	Zn^{2+}	none	benzene	46	58.7	13.0	28.3			
4	Al^{3+}	none	benzene	50	50.0	14.0	36.0			
5	$MgBr^+$	$ZnCl_2$ (0.5)	benzene	79	52.0	17.8	24.7	4.1	1.4	
6	$MgBr^+$	$SnCl_4$ (1.0)	benzene	79	75.9	8.9	15.2			
7	$MgBr^+$	$AlCl_3$ (0.3)	benzene	45	64.4	15.6	20.0			
8	$MgBr^+$	THF	benzene	14	85.7	7.1	14.2			
9	$MgBr^+$	glyme	benzene	6	100.0					
10	$MgBr^+$	none	toluene	87	51.8	12.6	26.4	4.6	3.4	1.2
11	$MgBr^+$	none	xylene	81	50.6	14.8	25.9	4.9	2.5	1.2

[a] Reaction time, 20 h; temperature, 80 ± 1 °C; phenol:aldehyde ratio, 2:1; concentration of metal phenolate was 0.3 M in all experiments. [b] Isolated yields based on phenol charged. [c] Determined by HPLC.

oligomers was performed by column chromatography on silica gel by using hexane/acetone solvent systems. Table I summarizes analytical and physical data of the obtained pure oligomers and reports the HPLC retention times in standard isocratic conditions and TLC retard factors (R_f) on silica gel plates. Expectedly, the elution order of the oligomer series in the reverse-phase HPLC (methanol/water) and in the silica gel chromatography using hexane/acetone as the eluent mixture follows the molecular size of the oligomer, while in the silica gel chromatography using chloroform as eluent a complete reversal is observed, as large oligomers elute faster than small ones.

A representative series of phenol–acetaldehyde condensation experiments was further selected to evaluate the effects of the phenolate metal counterion, the solvent, and the additives on yield, selectivity, and composition of the obtained resins. The main results are listed in Table II.

On inspection of these results it can be seen that the optimum conditions (yield >90%, ortho specificity ≥98%) were obtained at 80 °C with bromomagnesium salts in benzene (experiment 1). Among the other tested metal phenolates, only zinc and aluminum phenolates (experiments 3 and 4) showed appreciable reactivity, while alkali metal salts (experiment 2) were quite inert in refluxing benzene.

Furthermore, of the several Lewis acid cocatalysts added to the bromomagnesium phenolate (experiments 5–7), none of these appreciably affected the yield and the composition of the resin, while donor additives such as ethers (experiments 8 and 9) always blocked the reaction.[8] Use of aromatic hydrocarbon solvents other than benzene (experiments 10 and 11) as well as temperature and concentration variations had no apparent effects on the course of the phenol–acetaldehyde condensation, and the produced resins were almost identical in composition with a **3r:3m** ratio of ca. 2:1 and a **4mr:4rr** ratio of ca. 3:2.

Finally, two additional experiments were carried out with 1,1-diethoxyethane and paraldehyde as reagents, but, compared to the acetaldehyde reactions, only slight variations in yield and molecular composition of the resin were observed.

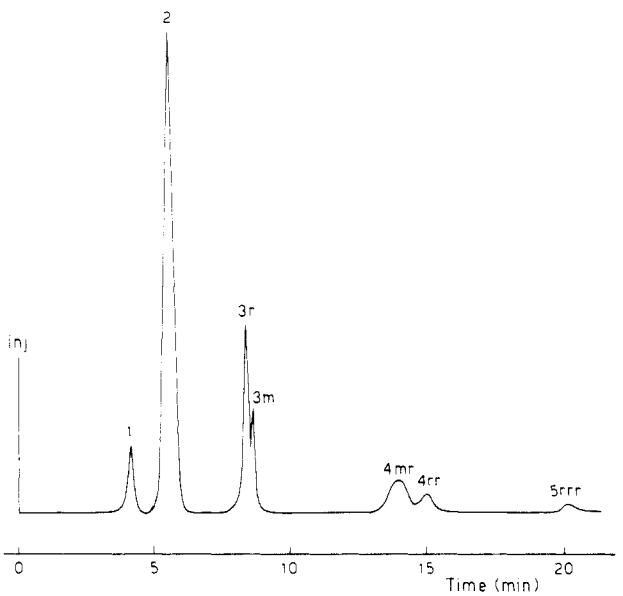

Figure 1. Reverse-phase HPLC profile of a typical all-ortho phenol–acetaldehyde novolac resin (experiment 1 in Table II). For conditions and peak identities, see text.

These first data indicate that bromomagnesium ion can effeciently promote the ortho-specific condensation of phenol with acetaldehyde or its derivatives and also hold promise that the stereochemical course of the reaction may be controlled by a careful choice and calibration of the metal promoters and the reagents.

Rational Synthesis of Regular Oligomers. The rational construction of linear ortho–ortho′ ethylidene-linked

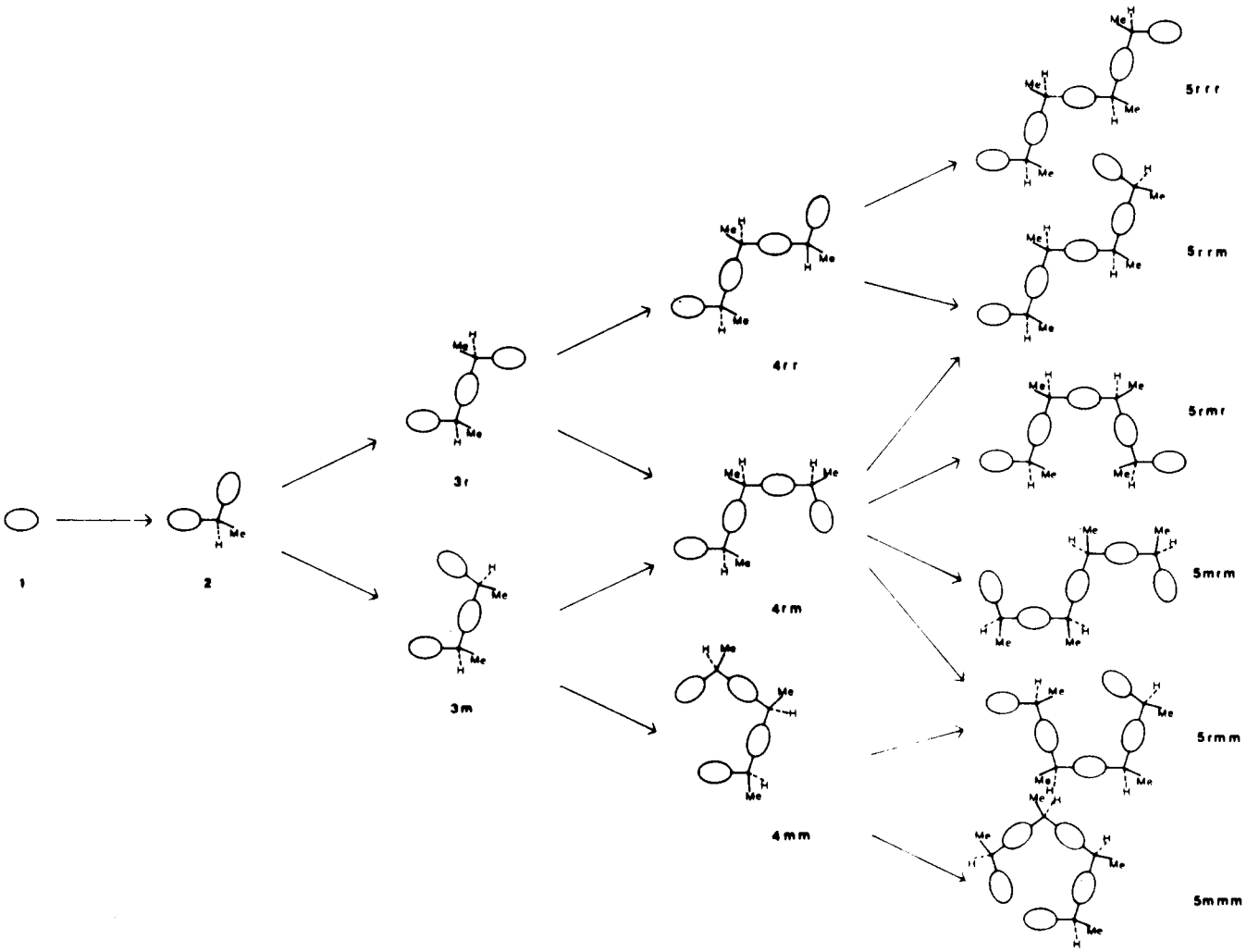

Figure 2. Phenol–acetaldehyde polycondensation reaction: competitive paths and oligomer stereosequences. Ellipses denote phenolic rings.

oligophenols was attempted by the same method used in our recently published syntheses of phenol–formaldehyde[3] and *p-tert*-butylphenol–formaldehyde[1] oligomers. Let us briefly recapitulate the strategy.

As exemplified in Scheme I, reaction A (hydroxybenzylation) is the reaction of a bromomagnesium salt of a suitable phenolic precursor with *rac*-2-hydroxy-α-methylbenzyl alcohol (**6**), leading to an oligomer containing one more phenolic unit, whereas reaction B (duplication) consists of the insertion of an ethylidene bridge between two equal phenolic synthons with acetaldehyde (**7**) or its derivatives (paraldehyde (**8**) or 1,1-diethoxyethane (**9**)), giving an oligomer twice the size of the starting one.

In this section we describe our attempts to selectively synthesize trinuclear, tetranuclear, and pentanuclear oligomers by using A and, occasionally, B routes.

Figure 2 gives a simplified picture of the possible pathways (up to pentanuclear compounds) of the ortho-specific step-growth polymerization of phenol (**1**) with *rac*-2-hydroxy-α-methylbenzyl alcohol (**6**), illustrating the stereosequence of the produced oligomers.

A. Binuclear Oligomer. We selectively synthesized **2** following reaction A. Thus, reaction of the bromomagnesium salt of phenol (**1**) in anhydrous benzene with an equimolecular amount of the bis(bromomagnesium) salt of *rac*-2-hydroxy-α-methylbenzyl alcohol (**6**) gave rise to **2** in 70% isolated yield.

Advantageously, it is also possible to obtain directly pure **2** in large amounts from the phenol–acetaldehyde resins of this study by recrystallization from benzene.

Scheme I
Rational Synthetic Access to Regular All-Ortho Ethylidene-Linked Polyphenols

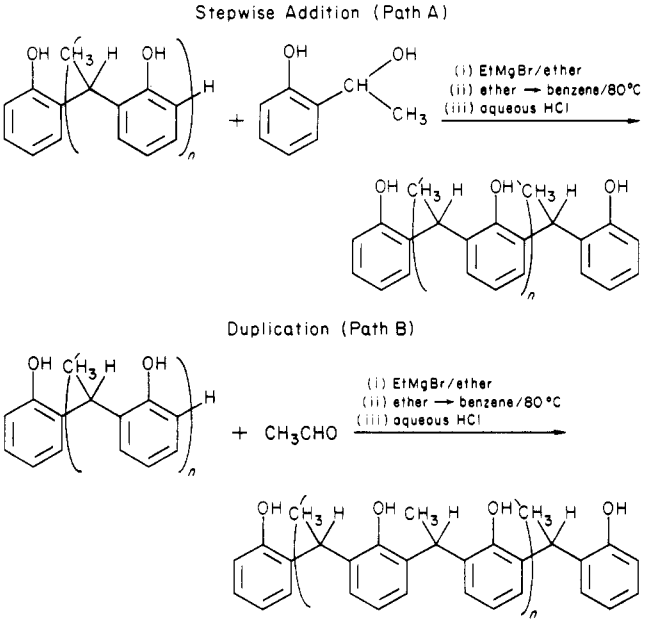

B. Trinuclear Oligomers. The procedure by which we attempted to synthesize **3r** and **3m** called for refluxing

Table III
Synthesis of Trinuclear Diastereoisomers Using Procedure A

expt	equiv of EtMgBr	product yield,[a] % 3m	3r	3m:3r ratio
1	2.0	7	42	14:86
2	2.5	14	31	31:69
3	3.0	22	23	49:51
4	3.5	25	11	69:31
5	4.0	27	3	89:11

[a] Isolated yield; the ramainder to 100% is due to unreacted starting compound and higher oligomers.

Table IV
Synthesis of Tetranuclear Diastereoisomers Using Procedures A and B

expt	reactants	equiv of EtMgBr	product yield,[a] % 4rm	4rr	4rm:4rr ratio
1	3r + 6	4	11	10	52:48
2	3r + 6	2	29	12	71:29
3	3m + 6	4	16		
4	3m + 6	2	34		
5	2 + 7	2	13	12	53:47
6	2 + 8	2	12	11	52:48
7	2 + 9	2	5	48	9:91

[a] See Table III.

bromomagnesium salts of **2** with equimolecular amounts of **6** in benzene solution.

In principle, the additional 2-hydroxy-α-methylbenzyl moiety could enter into **2** with its methyl group on the same side of the methyl of the existing bridge (syn mode) or on the opposite side (anti mode), generating meso and racemic diastereomeric dyads **3m** and **3r** as an equimolecular mixture. Rather fortunately, the extent of the salification of the hydroxyl functions of the reactants remarkably affected the stereochemical course of the reaction as seen in Table III.

When 2 mol equiv of ethylmagnesium bromide was employed to produce the phenolic salts, **3r** was obtained in 42% yield accompanied by only a 7% yield of **3m**, while use of 4 mol equiv of ethylmagnesium bromide (stoichiometric salification of the reactants) under otherwise identical conditions resulted in reversal of stereochemistry, and **3m** was the principal component in the condensate (40% yield).

The separation and purification of the diastereoisomers **3r** and **3m** were easily achieved by column chromatography (silica gel, hexane with increasing acetone) and recrystallization of the appropriate crude product as previously described for separation of the resin components.

C. Tetranuclear Oligomers. Both reactions A and B were attempted as a synthesis of compounds **4**, using **3m**, **3r**, and **2** as starting points. Since we have demonstrated that bromomagnesium salts of **2** and **3** are stable under our reaction conditions and no isomerization **3m** $\rightleftharpoons$ **3r** occurs, we tested five synthetic strategies: **3r** + **6** (Table IV, experiments 1 and 2), **3m** + **6** (experiments 3 and 4), **2** + **7** (experiment 5), **2** + **8** (experiment 6), and **2** + **9** (experiment 7).

Inspection of the data in Table IV first reveals that the stereochemical course of the reactions of both *meso*- and *rac*-**3** with **6** is only moderately controlled by the extent of the salification of the reactants, giving a prevalence of the atactic isomer **4mr** in all the experiments. In no case, however, did we find favorable conditions for the production of isotactic tetramer **4mm**. However, it is interesting to note that, in contrast to what is observed in the synthesis of trinuclear compounds, the amount of the syndiotactic oligomer **4rr** increases as the salification extent of the reactants is increased.

Nevertheless, a remarkable control in stereoselection was reached with duplication procedure B. While duplication of **2** with acetaldehyde itself (**7**) or paraldehyde (**8**) gave rise to a near 1:1 mixture of **4mr** and **4rr**, the analogous reaction with acetaldehyde diethyl acetal (**9**) leads to syndiotactic **4rr** preferentially in 48% yield and 91% selectivity.

As for compounds **3**, the separation of pure tetranuclear oligomers was performed by column chromatography on silica gel using hexane/acetone solvent mixtures.

D. Pentanuclear Oligomers. Among the six possible all-ortho pentanuclear diastereoisomers, we only succeeded in synthesizing **5rrr** by growth of **4rr** with **6**. Starting from **4rr**, using 4 mol equiv of ethylmagnesium bromide to salify the reactants in refluxing benzene, we obtained after routine workup a colorless solid product that showed two major peaks in HPLC, assigned to unreacted **4rr** (80%) and to pentanuclear compound **5rrr** (16%). A side product (1%) was also present, probably due to atactic **5rrm** diastereoisomer. Small-scale preparative liquid chromatography on a μ-Bondapak C-18 column using 80:20 (v/v) methanol/water as eluent afforded pure **5rrr** in 12% isolated yield.

Characterization of the Oligomers. Analytically pure samples of **2**, **3r**, **3m**, **4rm**, **4rr**, and **5rrr**, synthesized and separated as described in the preceding sections, were obtained by recrystallization from the solvents reported in Table I. The purity of individual compounds can be ascertained by the sharpness of their melting points, by thin-layer chromatography, by HPLC, and by ^{13}C NMR analyses.

A. IR, UV, and Mass Spectra. Significant IR, UV, and mass spectroscopic data of the six oligomers of this study are reported in Tables V and VI.

The IR spectra[9] taken as a solid mull, are closely similar within themselves, showing broad, very intense absorption bands at 3200–3340 cm^{-1} due to the intermolecular hydrogen-bonded hydroxyl vibrations (polymeric association) and sharp strong bands at 1220 and 1240 cm^{-1} (C–OH stretching) and near 760 cm^{-1} (C–H aromatic bending). In addition, three characteristic bands at 1600, 1490, and 1460 cm^{-1} and one sharp band of medium intensity near 2980 cm^{-1} are also present in all the spectra, assigned to C=C

Table V
IR and UV Spectral Data for Prepared Oligomers

compd	IR (KBr), cm^{-1} OH	C=C	C–O	C–H	UV (95% ethanol), nm (ϵ, cm^2/mol)
2	3200	1595, 1490, 1455	1225, 1125	755	281 (5135), 275 (5431)
3r	3280	1600, 1490, 1460	1240, 1125	760	281 (6850), 276 (6978)
3m	3260	1585, 1490, 1455	1220, 1120	755	281 (6781), 275 (7013)
4rm	3320	1590, 1490, 1455	1240, 1120	755	281 (8750), 276 (8697)
4rr	3300	1595, 1490, 1455	1235, 1125	750	281 (9714), 275 (9597)
5rrr	3340	1590, 1490, 1455	1240, 1125	755	281 (11077), 276 (10876)

Table VI
Mass Spectral Data for Prepared Oligomers

compd	mass spectrum, *m/e* (rel intens)[a]
2	214 (60), 199 (62), 181 (15), 166 (6), 152 (21), 121 (100), 120 (34), 94 (11), 91 (36), 77 (24), 65 (15)
3r	334 (32), 319 (8), 241 (8), 240 (34), 225 (36), 214 (12), 199 (11), 181 (8), 166 (8), 152 (7), 147 (20), 132 (9), 121 (100), 120 (10), 107 (10), 102 (12), 94 (11), 91 (18), 77 (17), 65 (8)
3m	334 (44), 319 (9), 241 (9), 240 (41), 225 (44), 214 (13), 199 (11), 181 (100), 166 (5), 152 (7), 147 (22), 132 (9), 121 (100), 120 (11), 107 (11), 102 (12), 94 (11), 91 (18), 77 (16), 65 (6)
4mr	454 (44), 439 (4), 361 (3), 360 (9), 345 (6), 334 (10), 319 (3), 266 (10), 241 (41), 240 (79), 225 (26), 214 (13), 199 (6), 181 (4), 166 (4), 147 (58), 132 (9), 121 (100), 120 (9), 107 (12), 102 (12), 94 (6), 91 (15), 77 (10), 65 (9)
4rr	454 (22), 439 (3), 361 (2), 360 (6), 345 (4), 334 (6), 319 (3), 266 (7), 241 (27), 240 (51), 225 (29), 214 (7), 199 (7), 181 (7), 166 (9), 147 (56), 132 (12), 121 (100), 120 (10), 107 (13), 102 (17), 94 (25), 91 (28), 77 (20), 65 (6)
5rrr	574 (4), 559 (1), 480 (1), 454 (3), 439 (1), 361 (3), 360 (10), 345 (4), 334 (6), 319 (5), 266 (12), 241 (32), 240 (44), 225 (23), 214 (12), 199 (12), 181 (5), 166 (4), 147 (73), 132 (12), 121 (100), 120 (15), 107 (9), 102 (12), 94 (12), 91 (20), 77 (12), 65 (6)

[a] At 70 eV; ionization chamber temperatures: 2, 110 °C; 3r and 3m, 190 °C; 4rm and 4rr, 240 °C; 5rrr, 290 °C.

phenyl ring stretching and methyl vibrations, respectively. The increase of the oligomer size from **2** to **5** results in an appreciable upward frequency shift of the hydroxyl band, probably ascribed to diminished polymeric association of higher oligomers. Furthermore, comparison of the IR spectra of *meso*- and *rac*-**3** and syndiotactic and atactic **4** diastereoisomers reveals such close similarities that any measurement is a fruitless exercise.

In the electronic spectra,[10] the six ethylidene-linked polyphenols of this study display two close absorption bands at 275 and 281 nm, arising from $\pi \rightarrow \pi^*$ transitions (B bands). As for the methylene-linked polyphenol series,[3] a linear dependence of the molar absorptivity for ethanol solutions at 281 nm upon the number of aromatic units in the oligomers was observed ($\epsilon = 1807n + 1510$), showing a very similar trend. Since no significant differences in the two lines were observed, one can say that modification of the bridging structure from methylene to ethylidene scarcely affects aromatic transitions.

In the mass spectra, all the oligomers give the corresponding molecular ion peak and show a gradual decline in the abundance of fragments with increasing fragment weight. The base peak in all the spectra at *m/e* 121 likely corresponds to 2-hydroxy-α-methylbenzyl ion ($C_8H_9O^+$), arising from simple benzylic cleavage of an external ethylidene bridge. The fragmentation pattern of this class of compounds is characterized by peaks of the even-ion series $C_{8n-2}H_{8n-2}O_n^+$ at *m/e* 574, 454, 334, and 214 corresponding to the mass of the single oligomers arising from a McLafferty-type hydrogen rearrangement with charge retention and cleavage of an external bridge (loss of a C_8H_8O neutral molecule).

In addition, peaks in the series $C_{8n}H_{8n}O_n^+$ are also prominent at *m/e* 480, 360, 240, etc., generated from the above series by H rearrangement, charge migration, and loss of a neutral phenol molecule (94 mass units apart). Other fragments are due to ions derived from the C–CH_3 σ-bond dissociation (15 mass units apart) at *m/e* 559, 439, 319, etc.

Unfortunately, as in the IR analysis mass spectroscopy under our experimental conditions (70 eV) on trinuclear and tetranuclear diastereoisomers exhibits no systematic variation and provides no valuable stereochemical information.

B. ^{13}C and ^1H NMR Studies. By combining the results obtained by spectroscopic analysis, mainly NMR, and by X-ray analysis, we have been able to gain a rather detailed understanding of the stereochemistry of these compounds.

The ^{13}C and ^1H chemical shifts of the examined oligomers are reported in Tables VII and VIII, respectively.

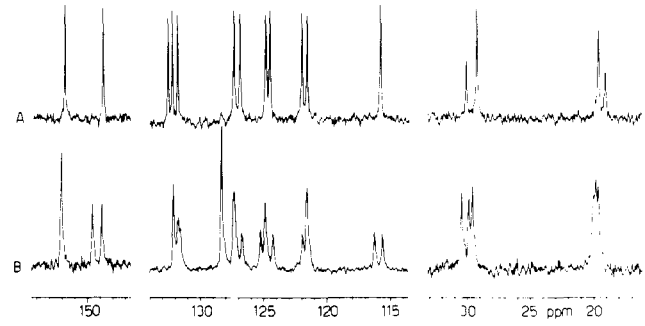

Figure 3. Proton-noise-decoupled ^{13}C NMR spectra of diastereomeric compounds **4rr** (A) and **4rm** (B).

The ^{13}C NMR spectra of the compounds **4rr** and **4rm** are reported in Figure 3.

The assignment of the individual lines to the different carbon atoms was obtained with the usual spectroscopic means and by comparing the spectra of the analogous oligomers deriving from phenol–formaldehyde condensation[11] and of model compounds such as 2-isopropyl- and 2,6-diisopropylphenol. As a general rule, each symmetric oligomer shows $n/2 + 1$ signals, where n is the total number of carbons. Moreover, in the presence of a plane of symmetry through the COH and the para carbon or an axis of symmetry through the internal ethylidene bridge, the intensity of the carbon lines corresponds to one atom only, while the intensity of the other carbon lines corresponds to two carbons.

Regarding the proton spectra, only the aliphatic region contains valuable information on the molecular symmetry or dissymmetry of the oligomers, since at 100 MHz the aromatic region is too complex to be analyzed.

C. X-ray Analysis. Bond distances, bond angles, and selected torison angles of the two diastereomeric compounds **3m** and **3r** are practically equal in the two examined compounds and are as expected for these systems, with insignificant deviations from average values obtained from literature data.[12] On the other hand, the conformations of these two molecules require a deeper discussion, in order to deduce some general aspects that could let us postulate some common rules that may be valid for all the compounds of this series, on the grounds also of the solid-state conformations of the di-, tri-, and tetranuclear phenol–formaldehyde oligomers previously reported.[3]

In Figures 4 and 5 are shown projections of the two molecules seen along the C(7)···C(7)′ directions passing through the two ethylidene bridges and along the C(4)···C(1)–O(1) directions of the internal rings, respectively. As can be noted, **3r** shows an anti conformation (chairlike),

Table VII
^{13}C NMR Data and Assignments for Prepared Oligomers

	^{13}C NMR ($CDCl_3$, Me_4Si), δ [a]											
	aliphatics				aromatics							
	CH_3		CH		CH	CH para		CH	C	COH		
compd	int	ext	ext	int	ortho	ext	int	meta	ortho'	int	ext	
2	19.42		29.36		115.68	121.45		126.82 127.20	131.41	151.73		
3r	19.58		29.39		115.94	121.68		124.21 127.09	131.99	149.03	151.36	
3m	19.71		29.31		115.29	121.35	121.80	124.73 126.31 127.21	131.17 131.72	148.63	151.50	
4mr	19.57	19.77 19.90	29.58 29.91	30.46	115.54 116.16	121.54	121.95	124.30 124.88 125.28 126.76 127.34 128.32	131.54 131.69 131.79 132.13	148.90 149.62	152.10	
4rr	19.06	19.61	29.31	30.16	115.62	121.50	121.95	124.50 124.82 126.84 127.31	131.74 132.17 132.52	148.89	151.90	
5rrr	19.73		29.54	29.91	115.75	121.36	121.76	124.54 126.92 127.05	131.77 132.17 132.35 132.47	148.63 148.99	151.91	

[a] At 25.16 MHz and 27 ± 1 °C; concentration ca. 10% (w/v).

Table VIII
^{1}H NMR Data and Assignments for Prepared Oligomers

	^{1}H NMR ($CDCl_3$, Me_4Si), δ [a]			
compd	$CHCH_3$	$CHCH_3$	aromatics	OH
2	1.63 (d, 3 H)	4.71 (q, 1 H)	6.6-7.5 (m, 8 H)	7.44 (s, 2 H)
3r	1.61 (d, 6 H)	4.77 (q, 2 H)	6.7-7.5 (m, 11 H)	8.04 (br s, 3 H)
3m	1.68 (d, 6 H)	4.78 (q, 2 H)	6.3-7.5 (m, 11 H)	8.56 (br s, 3 H)
4mr	1.52 (d, 3 H) 1.55 (d, 3 H) 1.65 (d, 3 H)	4.56 (q, 1 H) 4.69 (q, 1 H) 4.76 (q, 1 H)	6.6-7.5 (m, 14 H)	7.57 (br s, 4 H)
4rr	1.67 (d, 9 H)	4.70 (q, 1 H) 4.85 (q, 2 H)	6.3-7.5 (m, 14 H)	8.58 (br s, 4 H)
5rrr	1.48 (d, 6 H) 1.59 (d, 6 H)	4.73 (q, 4 H)	6.3-7.5 (m, 17 H)	8.50 (br s, 5 H)

[a] At 100 MHz and 27 ± 1 °C; concentration ca. 15% (w/v).

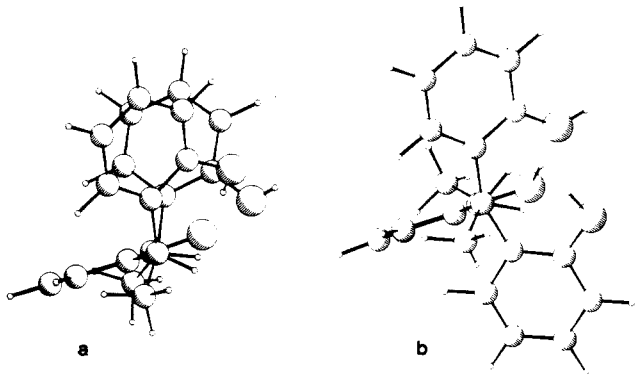

Figure 4. Projections of the molecules along the C(7)···C(7)′ direction: (a) compound **3m**; (b) compound **3r**.

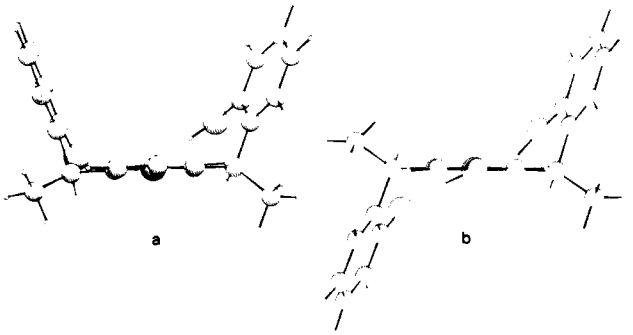

Figure 5. Projections of the molecules along the C(4)···C(1)–O(1) direction of the internal phenolic ring: (a) compound **3m**; (b) compound **3r**.

in the sense that the two external phenolic rings (1,3) are placed in an anti position; so it is similar to the trinuclear phenol–formaldehyde oligomer.[3] We can observe a completely opposite conformation in **3m**, in which the two external phenolic rings (1,3) are disposed in a syn position (quasi-eclipsed, boatlike).

In the solid state the conformation of both molecules is mainly determined by the intramolecular hydrogen-bond system involving the hydroxy groups. This is an isodromic system, each hydroxyl being a donor and an acceptor at the same time in an ordered sequence, and never doubly an acceptor. In the two compounds this characteristic is clearly pointed out by the O···O intra- and intermolecular distances given together with the other geometrical parameters of the hydrogen bond in Table IX.

It has already been proved that the isodromic hydrogen-bond system with the formation of infinite chains by

Table IX
Intramolecular and Intermolecular Hydrogen Bonding in Compounds 3r and 3m (in Å or Deg)

3r	3m
Intramolecular Bonding	
O(1)′-H(01)′ = 1.106 (37)	O(1)-H(01) = 1.023 (46)
O(1)′···O(1) = 2.790 (6)	O(1)···O(1)′ = 2.739 (3)
H(01)′···O(1) = 1.688 (37)	H(01)···O(1)′ = 1.723 (47)
O(1)′-H(01)′···O(1) = 173 (3)	O(1)-H(01)···O(1)′ = 171 (4)
O(1)″-H(01)″ = 1.135 (42)	O(1)′-H(01)′ = 0.996 (44)
O(1)″···O(1)′ = 2.705 (6)	O(1)′···O(1)″ = 2.751 (4)
H(01)″···O(1)′ = 1.665 (45)	H(01)′···O(1)″ = 1.769 (44)
O(1)″-H(01)″···O(1)′ = 150 (4)	O(1)′-H(01)′···O(1)″ = 168 (4)
Intermolecular Bonding[a]	
O(1)-H(01) = 1.012 (43)	O(1)″-H(01)″ = 0.938 (48)
O(1)···O(1)″^{i} = 2.726 (6)	O(1)″···O(1)^{i} = 2.745 (4)
H(01)···O(1)″^{i} = 1.714 (43)	H(01)″···O(1)^{i} = 1.815 (48)
O(1)-H(01)···O(1)″^{i} = 178 (4)	O(1)″-H(01)″···O(1)^{i} = 171 (4)

[a] i = $-x + 1, -y + 1, -z$.

cooperative effects contributes significantly to the stabilization of the system.[13]

However, in order to explain the reason why **3m** presents a syn conformation and **3r** an anti conformation, we must take into account the oligomer stereosequence, that is, the reciprocal arrangement of the methyl groups and the spatial array of the methyl groups with respect to the hydrogen-bond system. As is evident from Figure 4, since the presence of a methyl group along the O–H···O direction would lead to a destabilization of the molecule, the hydrogen-bond system must always run in the region of less steric hindrance in the molecule, i.e., the side opposite to that of the methyl groups. Thus, the anti and syn conformations of **3r** and **3m** are the only possible arrangements that allow such a favorable situation.

Having established that preferential conformations are those in which the hydrogen-bond system runs on the opposite side with respect to the methyl groups, we may formulate a general rule regarding the qualitatively more stable conformations for the oligomers of this class on the basis only of their stereosequence; that is: *Staggered conformations (anti) of the external phenolic rings correspond to racemic dyads, while eclipsed conformations (syn) correspond to meso dyads.*

As a consequence of this rule, we may hypothesize the conformation in the solid state of the three tetranuclear diastereoisomers **4mm**, **4mr**, **4rr** and of the pentanuclear diastereoisomer **5rrr**, of which suitable crystals for X-ray purposes have not yet been obtained. we can postulate with some confidence a protocyclic syn–syn conformation rather sterically constrained for **4mm** (this fact would explain the difficulty in synthesizing this compound), two meso dyads being present in the molecule, a syn–anti (anti–syn) conformation for **4mr** (**4rm**) similar to that of the tetranuclear phenol–formaldehyde oligomer,[3] an anti–anti conformation for **4rr**, since two racemic dyads are present, and finally an anti–anti–anti conformation for **5rrr**.

As observed in the phenol–formaldehyde trinuclear oligomer,[3] in the solid state the molecules are joined in centrosymmetric cyclic dimeric units by intermolecular hydrogen bonding (see Table IX). Figures 6 and 7 show a [001] packing diagram for compound **3m** and a [100] packing diagram for compound **3r**, respectively. Other contacts are consistent with van der Waals interaction radii.

Conclusions

We have reported herein a high-yield synthesis of all-ortho acetaldehyde novolacs (ethylidene-linked polyphenols) from phenol and acetaldehyde (or paraldehyde or 1,1-diethoxyethane). Preferential racemic dyad arrangements over meso dyads in the polycondensation mixtures were found, using bromomagnesium, zinc, and aluminum phenolates in nonprotic apolar solvents.

A versatile route leading to the synthesis of individual regular oligomers (from dinuclear to pentanuclear) has also been developed by the growth of suitable phenolic precursors with *rac*-2-hydroxy-α-methylbenzyl alcohol. Complete regiochemical control of these processes was achieved with bromomagnesium phenolates in refluxing benzene.

Reversal in stereochemistry in the growth reactions of **2** with 2-hydroxy-α-methylbenzyl alcohol (**6**) was observed according to the salification extent of the reactants, leading to viable stereospecific syntheses of **3m** and **3r**. Stereo-

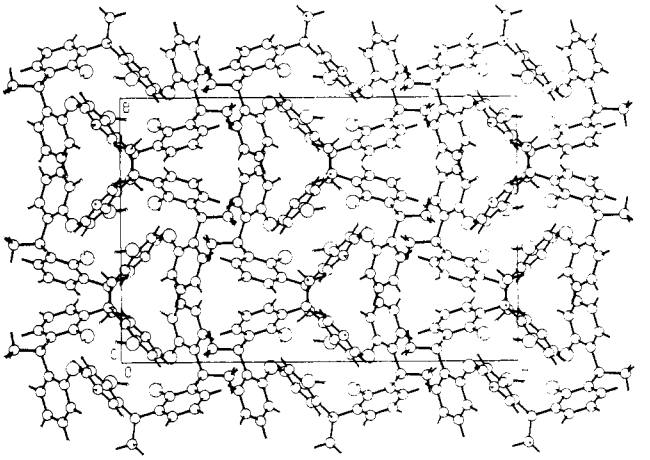

Figure 6. Compound **3m**. Molecular packing seen along [001].

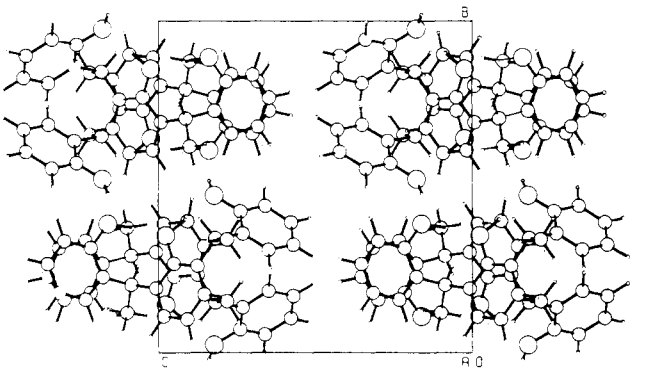

Figure 7. Compound **3r**. Molecular packing seen along [100].

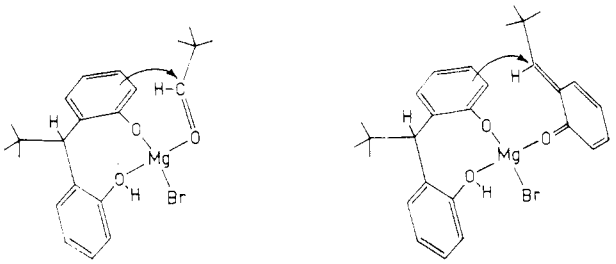

Figure 8. Possible steric arrangements of the reacting molecules in template-like transition states: (left) hydroxyalkylation step; (right) hydroxybenzylation step.

controlled synthesis of tetranuclear compound **4rr** (91% syndiospecificity) was also achieved by duplication of **2** with acetaldehyde diethyl acetal (**9**).

Although a complete rationale for the described processes on the sole basis of the synthetic and structural results of this study is hard to construct, let us formulate some mechanistic hypotheses to account for the regio- and stereochemical reaction behavior.

As regards the reaction regiospecificity, we wish once more to emphasize the unique role played by the bromomagnesium ion in directing aromatic substitution ortho specifically.[5,14] Although no direct evidence is yet available, we can suppose that the magnesium atom located at the phenolic hydroxyl coordinates electrophilic species, generating donor–acceptor intermediate complexes responsible for both the activation and orientation of reaction partners. In other words, acetaldehyde or the quinone methide intermediate that likely arises from salicyl alcohol by bromomagnesium phenoxide catalyzed dehydration rapidly reacts with the phenolic ortho carbon by virtue of their proximity to this side of the aromatic ring as seen in Figure 8.

Furthermore, the dramatic dependence of the **3m:3r** diastereomeric ratio upon the amount of magnesium employed in reactions of **2** with **6** could be rationalized by assuming preferential steric arrangements of involved transition states or a different template assistance exerted by the coordinating magnesium ion.[15]

This study has once more pointed out that, among spectroscopic methods, combined ^1H and ^{13}C NMR is the most useful diagnostic technique for the configurational analysis of phenol–aldehyde oligomeric compounds. Although useful information such as molecular size and symmetry may be obtained, this technique alone or in combination with usual IR, UV, and mass spectroscopy does not provide sufficient information for unambiguous differentiation of symmetric molecules with the same size (e.g., **3m** and **3r**). Hence, single-crystal X-ray structural analysis appears to be an indispensable tool to solve this structural problem.

Furthermore, the X-ray analysis of diastereomeric trinuclear derivatives **3m** and **3r** has pointed out the key role played by the intra- and intermolecular hydrogen bonding and by the mutual interaction between the H-bond system and the bridging ethylidenes in determining the solid-state conformational arrangement of a single molecule as well as its polymeric association in the crystal.

Experimental Section

General Methods. The instrumentation and procedures employed in the HPLC measurements and the IR, UV, mass, ^1H NMR, and ^{13}C NMR analyses were given in our previous publication.[3] However, for chromatographic separations chloroform or hexane/acetone solvent mixtures were employed.

Materials. Phenol, ethyl bromide, benzene, and magnesium turnings were purchased from Carlo Erba, Milan, 2-hydroxyacetophenone and 1,1-diethoxyethane from Merck-Schuchardt, and acetaldehyde and paraldehyde from Fluka A.G., Buks. Other chemicals and solvents were also commercially available and were used without further purification. *rac*-2-Hydroxy-α-methylbenzyl alcohol was prepared by $NaBH_4$ reduction of 2-hydroxyacetophenone in methanol solution. Sodium, potassium, and aluminum phenolates were prepared from phenol and the corresponding finely dispersed metals in refluxing benzene, lithium phenolate was prepared from phenol and *n*-butyllithium, and zinc phenolate was prepared from phenol and diethylzinc in benzene.

Table X
Crystal Data for Compounds 3m and 3r

	3m	3r
formula	$C_{22}H_{22}O_3$	$C_{22}H_{22}O_3 \cdot {}^1/_2C_6H_6$
M_r	334.40	334.40
crystal system	orthorhombic	monoclinic
space group	*Pbca*	$P2_1/a$
Z	8	4
a, Å	23.326 (7)	10.246 (4)
b, Å	15.287 (6)	14.588 (6)
c, Å	10.247 (4)	14.023 (6)
β, deg		96.25 (4)
V, Å^3	3654 (2)	2084 (2)
D_c, g cm^{-3}	1.216	1.190
radiation	Cu Kα	Cu Kα
temp, °C	22 ± 1	22 ± 1
final R value	0.049	0.083

Synthesis of All-Ortho Phenol–Acetaldehyde Novolac Resins. Typical Procedure. To a solution of ethylmagnesium bromide [prepared in situ from ethyl bromide (32.4 g, 0.3 mol) and magnesium turnings (7.2 g, 0.3 mol)] in diethyl ether (250 mL), a solution of phenol (28.2 g, 0.3 mol) in diethyl ether (100 mL) was added dropwise under stirring at room temperature. Most of the ether was removed under vacuum with gentle warming, and anhydrous benzene (350 mL) was added. The resulting slurry mixture was distilled until the temperature rose to 80 °C to remove the ether completely. After the mixture cooled, the volume was adjusted to 900 mL with benzene, and acetaldehyde (6.6 g, 0.15 mol) in benzene (100 mL) was added with stirring. The resulting yellow–ochre slurry mixture was refluxed for 20 h with vigorous stirring, quenched with 5% aqueous hydrochloric acid solution (600 mL), and then extracted three times with ether (300 mL each). The combined extract, dried over anhydrous sodium sulfate, was evaporated on a rotary apparatus to give 26 g (96% based on phenol) of a solid residue, mp 65–80 °C.

Other phenol–acetaldehyde condensation experiments listed in Table II were carried out in a suitably modified way as follows:

Experiments 2–4 in Table II: the acetaldehyde solution was added to the suitable metal phenolate in benzene directly.

Experiments 5–9 in Table II: the additives were added to the benzene solution of phenoxymagnesium bromide after solvent exchanging.

Experiments 10 and 11 in Table II: the appropriate solvent was used.

Preparative data and composition of all the prepared resins are listed in Table II.

Separation of Resin Components. Typical Procedure. The resin of the above preparation (10.0 g) was chromatographed on a silica gel column (1000 g) using hexane with increasing acetone as eluent. The single components were eluted in the following order: unreacted phenol **1** (acetone 50%), 1.4 g (14%); **2** (acetone, 5.6%), 4.7 g (47%); **3m** (acetone 6.2%), 1.0 g (10%); **3r** (acetone 6.5%), 2.3 g (23%); **4rm** (acetone 9.2%), 0.3 g (3%); **4rr** (acetone 10.4%), 0.25 g (2.5%); **5rrr** (acetone 11.3%), 0.15 g (1.5%).

Analytical and physical data of single pure oligomers are listed in Table I. Significant spectral data and assignments are reported in Tables V–VIII.

***meso*- and *rac*-2,6-Bis(2-hydroxy-α-methylbenzyl)phenol (3m and 3r). Typical Stepwise Reaction (Table IV, Experiment 1).** To a solution of ethylmagnesium bromide [prepared in situ from ethyl bromide (4.32 g, 0.04 mol) and magnesium turnings (0.96 g, 0.04 mol)] in diethyl ether (25 mL), a solution of 2,2′-ethylidenediphenol (**2**) (4.28 g, 0.02) and *rac*-2-hydroxy-α-methylbenzyl alcohol (**6**) (2.76 g, 0.02) in diethyl ether (60 mL) was added at room temperature. Most of the ether was removed

Table XI
3m: Atomic Coordinates for Non-Hydrogen Atoms ($\times 10^4$) and for Hydrogen Atoms ($\times 10^3$) with Estimated Standard Deviations in Parentheses

atom	*x/a*	*y/b*	*z/c*	atom	*x/a*	*y/b*	*z/c*
O(1)	5285 (1)	4271 (2)	1784 (3)	C(3)′	3724 (2)	2971 (2)	4430 (4)
O(1)′	4142 (1)	3967 (2)	1371 (3)	C(4)′	3163 (2)	3243 (3)	4552 (4)
O(1)″	3772 (1)	5206 (2)	−385 (3)	C(5)′	2913 (1)	3747 (2)	3581 (4)
C(1)	5375 (1)	4165 (3)	3122 (4)	C(6)′	3224 (1)	3994 (2)	2480 (3)
C(2)	5774 (2)	4714 (3)	3699 (4)	C(7)′	2960 (1)	4529 (2)	1374 (4)
C(3)	5888 (2)	4639 (3)	5022 (4)	C(8)′	2298 (2)	4482 (3)	1338 (5)
C(4)	5607 (2)	4015 (3)	5741 (4)	C(1)″	3548 (1)	5796 (2)	492 (4)
C(5)	5214 (2)	3470 (3)	5154 (4)	C(2)″	3158 (1)	5484 (2)	1408 (4)
C(6)	5090 (1)	3516 (2)	3818 (3)	C(3)″	2952 (2)	6067 (3)	2329 (5)
C(7)	4666 (1)	2900 (2)	3176 (3)	C(4)″	3122 (2)	6945 (3)	2329 (6)
C(8)	4752 (2)	1938 (2)	3613 (4)	C(5)″	3502 (2)	7229 (3)	1383 (6)
C(1)′	3795 (1)	3728 (2)	2410 (3)	C(6)″	3712 (2)	6670 (3)	455 (6)
C(2)′	4050 (1)	3198 (2)	3344 (3)				
H(01)	486 (2)	420 (3)	156 (4)	H(3)′	392 (1)	258 (1)	519 (1)
H(01)′	404 (2)	419 (3)	97 (4)	H(4)′	292 (1)	306 (1)	540 (1)
H(01)″	407 (2)	543 (3)	−90 (5)	H(5)′	274 (1)	396 (1)	368 (1)
H(2)	599 (1)	520 (1)	312 (1)	H(7)′	311 (1)	423 (1)	49 (1)
H(3)	620 (1)	506 (1)	548 (1)	H(81)′	22 (1)	379 (1)	127 (1)
H(4)	569 (1)	396 (1)	677 (1)	H(82)′	216 (1)	480 (1)	45 (1)
H(5)	499 (1)	299 (1)	574 (1)	H(83)′	206 (1)	475 (1)	216 (1)
H(7)	476 (1)	292 (1)	214 (1)	H(3)″	265 (1)	584 (1)	306 (1)
H(81)	519 (1)	175 (1)	339 (1)	H(4)″	296 (1)	739 (1)	305 (1)
H(82)	446 (1)	152 (1)	307 (1)	H(5)″	363 (1)	791 (1)	138 (1)
H(83)	467 (1)	186 (1)	465 (1)	H(6)″	400 (1)	691 (1)	−28 (1)

Table XII
3r: Atomic Coordinates for Non-Hydrogen Atoms ($\times 10^4$) and for Hydrogen Atoms ($\times 10^3$) with Estimated Standard Deviations in Parentheses

atom	*x/a*	*y/b*	*z/c*	atom	*x/a*	*y/b*	*z/c*
O(1)	4152 (4)	5243 (3)	1780 (3)	C(7)′	4368 (5)	7942 (4)	−870 (4)
O(1)′	3712 (3)	6454 (2)	239 (3)	C(8)′	5265 (7)	8785 (5)	−996 (7)
O(1)″	4041 (4)	6103 (3)	−1614 (3)	C(1)″	3434 (6)	6826 (5)	−2155 (5)
C(1)	4153 (5)	5717 (4)	2608 (4)	C(2)″	3540 (5)	7700 (4)	−1780 (4)
C(2)	5071 (6)	5560 (5)	3394 (5)	C(3)″	2815 (7)	8386 (5)	−2325 (5)
C(3)	5078 (7)	6054 (5)	4217 (5)	C(4)″	2054 (8)	8181 (7)	−3163 (6)
C(4)	4134 (8)	6722 (5)	4294 (5)	C(5)″	1991 (8)	7309 (7)	−3528 (6)
C(5)	3207 (6)	6876 (5)	3507 (5)	C(6)″	2675 (7)	6621 (6)	−2996 (5)
C(6)	3169 (5)	6384 (4)	2681 (4)	C(1B)	5581 (7)	10448 (4)	5818 (1)
C(7)	2134 (5)	6532 (4)	1814 (4)	C(2B)	5357 (7)	10228 (4)	4100 (1)
C(8)	728 (5)	6569 (6)	2182 (5)	C(3B)	4098 (7)	9295 (4)	5091 (1)
C(1)′	3222 (5)	7303 (4)	495 (4)	C(1B)′	5107 (1)	9162 (2)	4534 (3)
C(2)′	2433 (5)	7365 (4)	1241 (4)	C(2B)′	6160 (1)	10513 (2)	5257 (3)
C(3)′	1991 (6)	8229 (5)	1463 (5)	C(3B)′	3890 (1)	10196 (2)	5432 (3)
C(4)′	2245 (7)	8981 (5)	919 (5)	C(1B)″	5757 (1)	10116 (1)	5900 (0)
C(5)′	3013 (6)	8894 (4)	167 (5)	C(2B)″	5380 (1)	10799 (1)	4325 (0)
C(6)′	3514 (5)	8049 (4)	−76 (4)	C(3B)″	3578 (1)	10116 (1)	5047 (0)
H(01)	483 (4)	475 (3)	171 (3)	H(3)′	145 (1)	831 (1)	207 (1)
H(01)′	381 (3)	297 (2)	85 (3)	H(4)′	184 (1)	964 (1)	107 (1)
H(01)″	425 (5)	621 (2)	−81 (3)	H(5)′	323 (1)	950 (1)	−24 (1)
H(2)	579 (1)	502 (1)	336 (1)	H(7)′	505 (1)	739 (1)	−66 (1)
H(3)	583 (1)	393 (1)	480 (1)	H(81)′	591 (1)	888 (1)	−34 (1)
H(4)	411 (1)	710 (1)	495 (1)	H(82)′	465 (1)	938 (1)	−112 (1)
H(5)	249 (1)	742 (1)	355 (1)	H(83)′	585 (1)	869 (1)	−159 (1)
H(7)	215 (1)	596 (1)	132 (1)	H(3)″	286 (1)	908 (1)	−207 (1)
H(81)	5 (1)	661 (1)	154 (1)	H(4)″	150 (1)	872 (1)	−355 (1)
H(82)	62 (1)	717 (1)	262 (1)	H(5)″	143 (1)	716 (1)	−421 (1)
H(83)	52 (1)	596 (1)	258 (1)	H(6)″	259 (1)	592 (1)	−324 (1)

under vacuum, and anhydrous benzene (100 mL) was added. The resulting slurry was distilled until the temperature rose to 80 °C to remove the ether completely and then refluxed with stirring for 20 h, after the volume was adjusted to 200 mL with benzene. The yellow reaction mixture was quenched with an excess of a 5% aqueous hydrochloric acid solution and extracted three times with ether (100 mL each), and the combined organic layers were dried over anhydrous sodium sulfate. Removal of the solvent on a rotary apparatus gave a solid residue, which was chromatographed on preparative silica gel plates using hexane/acetone (80:20 (v/v)) as an eluent mixture to give pure **3m** [colorless microcrystals, yield 0.47 g (7% on **2**), mp 157–158 °C] and **3r** [colorless microcrystals, yield 2.80 g (42% on **2**), mp 120 °C].

Other stepwise reactions listed in Tables III and IV as well as those leading to the pentanuclear oligomer were carried out in a similar way using the appropriate phenolic precursor.

Atactic and Syndiotactic 6,6′-Bis(2-hydroxy-α-methylbenzyl)-2,2′-ethylidenediphenol (4rm and 4rr). Typical Duplication Reaction (Table V, Experiment 5). To a solution of ethylmagnesium bromide [prepared in situ from ethyl bromide (4.32 g, 0.04 mol) and magnesium turnings (0.96 g, 0.04 mol)] in diethyl ether (25 mL), a solution of 2,2′-ethylidenediphenol (**2**) (4.28 g, 0.02 mol) in diethyl ether (40 mL) was added with stirring at room temperature. After the ether was removed, benzene (100 mL) was added and the slurry was distilled until the temperature rose to 80 °C. After the mixture cooled, the volume was adjusted

to 190 mL with benzene, and then acetaldehyde (0.44 g, 0.01 mol) in benzene (10 mL) was added with stirring. The mixture was refluxed under stirring for 20 h and then quenched with an excess of a 10% aqueous hydrochloric acid solution. After the usual workup (extraction, drying, and removal of the solvent), preparative silica gel chromatography of the solid reaction residue using chloroform (stabilized with 0.3% w/v ethanol) as eluent gave **4rm** [colorless microcrystals, yield 0.59 g (13% on **2**), mp 155 °C] and **4rr** [colorless microcrystals, yield 0.54 g (12% on **2**), mp 165 °C.

Other duplication reactions reported in Table IV were performed in a similar way by using 1,1-diethoxyethane (experiment 7) or paraldehyde (experiment 6) as bridging reactants instead of acetaldehyde.

X-ray Analysis. Compound 3m. Colorless prismatic crystals were grown from a 5:1 hexane/acetone solution at room temperature. Preliminary lattice constants and the space group were determined from oscillation and Weissberg photographs. Precise cell parameters (from 29 high order reflections) and 3925 three-dimensional intensity data ($\pm h,k,l$, $2\theta_{max}$ = 139°) were measured on a General Automation GA Jumbo 220 controlled Siemens diffractometer with Ni-filtered Cu Kα (λ = 1.541 78 Å) radiation using the ω–2θ scan mode. Integrated intensities were obtained by using a profile-analysis program. The two reference reflections used for control and scaling of the intensities in the course of the data collection showed no significant variations. Crystal data are summarized in Table X. The structure was solved by direct methods. The atomic parameters were refined by a least-squares procedure, using anisotropic temperature factors. The hydrogen atoms attached to carbons were located in a ΔF map and included in the refinement with isotropic temperature factors. The OH hydrogen atoms were located in the final ΔF synthesis and not refined. The final R value ($R = \sum||F_o| - |F_c||/\sum|F_o|$) was 0.049 for the 2144 independent observed reflections ($I \geq 3\sigma(I)$) with a (number of observations)/(number of refined parameters) of 8.0. The average shift/error ratio at the end of the refinement was 0.012. The $|\Delta F|$ revealed a linear trend as a function of sin θ and of the magnitude of $|F|$. Fractional atomic coordinates are given in Table XI.

Compound 3r Benzene Clathrate. Crystals in the form of colorless plates were obtained from 1:1 benzene/cyclohexane solution. They spontaneously lose solvent, so they were sealed into a Lindeman capillary. Crystal data were determined as before and 4311 three-dimensional data ($\pm h,k,l$, $2\theta_{max}$ = 139°) were measured on the same diffractometer and with the same procedure. The reference reflection showed no significant variations. Crystal data are reported in Table X. The structure was solved by direct methods and refined by least squares using anisotropic parameters. The hydrogen atoms attached to carbons were included in the refinement with isotropic temperature factors and with the constraint of C–H = 1.08 Å. The OH hydrogen atoms were located in the final ΔF map and not refined. The benzene guest molecule was disordered in at least three orientations with the baricenter on the center of symmetry at $^1/_2$, 1.0, $^1/_2$, and it was refined as a rigid group. The refined occupancies were 0.520, 0.351, and 0.066 for the positions unprimed, primed, and double primed, respectively. The final R value was 0.070 for the 2387 independent observed reflections with a (number of observations)/(number of refined parameters) of 9.3. The average shift/error ratio at the end of the refinement was 0.020. The distribution of $|\Delta F|$ as a function of sin θ and of the magnitude of $|F|$ is mainly linear. The fractional coordinates are reported in Table XII. All the calculations were executed on a CDC Cyber 76 Computer (CINECA, Casalecchio, Bologna) and on a SEL 32/77 of the Institute using the SHELX system of programs.[16]

Acknowledgment. We acknowledge support of the Consiglio Nazionale delle Ricerche, Progetto Finalizzato Chimica Fine e Secondaria, and Prof. H. Kämmerer (University of Mainz, West Germany) for his encouragement throughout this work and for making ref 6 available to us. We also thank Mr. G. Zannoni for the measurements of some ^{13}C NMR spectra. We express our appreciation to the referees for helpful suggestions.

Registry No. **2**, 87804-18-0; **3m**, 87804-19-1; **3r**, 87804-20-4; **4mr**, 87804-21-5; **4rr**, 87860-10-4; **5rrr**, 87804-22-6; ethylmagnesium bromide, 925-90-6; 1,3,5-trioxane, 110-88-3; phenol, 108-95-2; acetaldehyde, 75-07-0; acetaldehyde diethyl acetal, 105-57-7; (±)-2-hydroxy-α-methylbenzyl alcohol, 87804-23-7.

Supplementary Material Available: Tables of bond distances, bond angles, selected torsion angles, and anisotropic thermal parameters and lists of observed and calculated structure factors for both structures (32 pages). Ordering information is given on any current masthead page.

References and Notes

(1) Part 2: Casiraghi, G.; Cornia, M.; Ricci, G.; Balduzzi, G.; Casnati, G.; Andreetti, G. D. *Makromol. Chem.* **1983**, *184*, 1363.
(2) (a) Istituto di Chimica Organica, Università di Parma. (b) Istituto di Strutturistica Chimica, Università di Parma. (c) Istituto di Chimica delle Macromolecole, CNR Milano.
(3) Casiraghi, G.; Cornia, M.; Sartori, G.; Casnati, G.; Bocchi, V.; Andreetti, G. D. *Makromol. Chem.* **1982**, *183*, 2611.
(4) Bender, H. L.; Farnham, A. G.; Guyer, J. W. U.S. Patent 2 464 207, 1948. Fraser, D. A.; Hall, R. W.; Raum, A. L. J. *J. Appl. Chem.* **1957**, *7*, 676. Peer, H. G. *Recl. Trav. Chim. Pays-Bas* **1960**, *79*, 825. Partansky, A. M. *Org. Coat. Plast. Chem.* **1967**, *27*, 115. Culberston, H. M. U.S. Patent 4 097 463, 1978.
(5) Casiraghi, G.; Casnati, G.; Pochini, A.; Ungaro, R. *J. Chem. Soc., Perkin Trans. 1* **1982**, 805.
(6) Kiegel, E. Ph.D. Dissertation, University of Mainz, Mainz, FRD, 1963. See also: Rothe, M. In "Polymer Handbook", 3rd ed.; Brandrup, J., Immergut, E. K., Eds.; Interscience: New York, 1967; Chapter VII, p 17.
(7) Cornia, M.; Sartori, G.; Casnati, G.; Casiraghi, G. *J. Liq. Chromatogr.* **1981**, *4*, 13.
(8) The ether effect in this reaction is similar to that observed in reactions involving alkylmagnesium derivatives: Caronne, P.; Foscolos, G.; Caron, H.; Lemay, G. *Tetrahedron* **1982**, *38*, 3563.
(9) Grisenthwaite, R. J.; Hunter, R. F. *J. Appl. Chem.* **1956**, 324. Cairns, T.; Eglinton, G. *Nature (London)* **1962**, *196*, 535.
(10) Hunter, R. F.; Morton, R. A.; Carpenter, A. T. *J. Chem. Soc.* **1950**, 441.
(11) Mukoyama, Y.; Tanno, T.; Yokokawa, H.; Fleming, J. *J. Polym. Sci.* **1973**, *11*, 3193. Dankelman, W.; Huysmans, W. G. B.; de Wit, J. *Angew. Makromol. Chem.* **1977**, *62*, 7. Dradi, E.; Casiraghi, G.; Casnati, G. *Chem. Ind. (London)* **1978**, 627. Dradi, E.; Casiraghi, G.; Sartori, G.; Casnati, G. *Macromolecules* **1978**, *11*, 1295. Sojka, S. A.; Wolfe, R. A.; Dietz, E. A., Jr.; Dannels, B. F. *Ibid.* **1979**, *12*, 767.
(12) Cambridge Crystallography Data Centre File. Allen, F. H.; Bellard, S.; Brice, M. D.; Cartwright, B. A.; Doubleday, A.; Higgs, H.; Hummelink, T.; Hummelink-Peters, B. G.; Kennard, O.; Motherwell, W. D. S.; Rodgers, J. R.; Watson, D. G. *Acta Crystallogr., Sect. B* **1979**, *35*, 2331. Barnes, J. C.; Paton, J. D.; Damewood, J. R., Jr.; Mislow, K. *J. Org. Chem.* **1981**, *46*, 4975.
(13) Schuster, P.; Karpfen, A.; Beyer, A. "Molecular Interaction"; Rataiczak, H.; Orville-Thomas, W. J., Eds.; Wiley: New York, 1980.
(14) Casnati, G.; Pochini, A.; Puglia, G.; Ungaro, R. *Tetrahedron Lett.* **1982**, *23*, 3803 and references therein.
(15) Further experimental work seems to be required to give a complementary development to the reaction mechanism.
(16) Sheldrick, G. M. In "Computing in Crystallography"; Schenk, H., Olthof-Hazekamp, R., van Koningsveld, H., Bassi, G. C., Eds.; Delft University Press: Delft, 1976; pp 34–42.